Program Digest, 2019 IEEE International Ultrasonics Symposium (IUS)
Glasgow, Scotland, October 6-9, 2019

In-vivo Validation of 3D Multi-frequency Liver Shear Wave Absolute Vibro-Elastography with an xMATRIX Array

Qi Zeng*, Mohammad Honarvar*, Julio Lobo*, Caitlin Schneider*, Shahed Mohammed*, Gerard Harrison†, Changhong Hu†, Scott Dianis‡, James Jago†, Robert Rohling*,and Septimiu E. Salcudean*
*Electrical and Computer Engineering, The University of British Columbia, Vancouver, BC Canada V6T 1Z4
†Philips Healthcare, Bothell, WA 98021 USA, ‡Philips, Andover, MA 01810 USA
Email:{tims,qizeng}@ece.ubc.ca

***Abstract*—Liver fibrosis arises from chronic liver diseases, such as hepatitis B, C and nonalcoholic steatohepatitis and can result in cirrhosis and death. Magnetic resonance elastography (MRE) is commonly regarded as the imaging-based gold-standard for fibrosis staging. With the aid of a state-of-the-art matrix array transducer, our previous 3D ultrasound shear wave absolute vibro-elastography (S-WAVE) imaging was able to generate hepatic stiffness measurements which are comparable to MRE. In this work, we introduce multi-frequency S-WAVE imaging with a matrix array transducer, to provide more robust and reliable measurements with a shorter overall exam time. The system was characterized with three liver tissue phantoms of different elasticity using the MRE results as the ground truth. Six healthy volunteers and six patients who have chronic liver diseases were imaged. Our results indicate that measurements from multi-frequency 3D S-WAVE with a matrix array transducer correlated better to MRE, compared to the readings from the transient elastography method (FibroScan, Echosens).**

I. Introduction

Over the last few decades, elastography has been gradually accepted by the clinical world as an effective imaging-based diagnosis tool as it provides quantitative viscoelasticity measurements of biological tissue. For the liver, elastography techniques have shown their potential in assessing tissue fibrotic conditions induced by chronic diseases, such as hepatitis B, C and nonalcoholic steatohepatitis. In existing clinical studies, magnetic resonance elastography (MRE) has shown promising results for fibrosis staging when using the liver biopsy result as the ground truth [1].

Cost-effective and easily accessible alternative elasticity imaging techniques based on ultrasound have been developed over the last two decades. Commercial products based on transient elastography (TE), acoustic radiation force impulse (ARFI)-based point quantification shear wave elastography (pSWE), and 2D shear wave imaging (2D SWI) are available for monitoring the patients' hepatic stiffness. However, the performance of these techniques in detecting early stage fibrosis and assessing very stiff tissue is limited, mainly because of the limited shear wave penetration and field-of-view (FOV) [2].

Our group has developed Shear Wave Absolute Vibro-elastography (S-WAVE), a technique which captures the volumetric shear wave pattern of the tissue while a multi-frequency mechanical excitation is applied externally [3]. In our most recent work, the volumetric acquisition was adapted to work with a matrix array transducer resulting a system that is capable of generating large FOV 3D elasticity imaging, and *in vivo* validation results for a small cohort of healthy volunteers ($n = 5$) was shown to be in good agreement with MRE measurements [4]. However, its performance and efficiency was still limited by the single frequency shear wave imaging setup.

In this work, multi-frequency 3D volumetric acquisition is implemented, allowing for S-WAVE imaging with the matrix array transducer. To achieve this, we used a customized color power angiography (CPA) scan sequence. We show that our system that is capable of providing more robust and reliable hepatic stiffness measurements with a shorter overall exam time. We characterized the measurements with three liver tissue phantoms of different elasticity, and further validated the system performance with a larger cohort of healthy volunteers and patients with chronic liver diseases.

II. Methods

A. Imaging System

In this implementation, our 3D S-WAVE imaging employs the EPIQ 7G ultrasound platform with an X6-1 xMATRIX array transducer (Philips Healthcare, Bothell, WA). The controlled shear wave excitation is provided by a shaker board placed underneath the patient's back. The research package provide by the EPIQ 7G platform is used to capture the radio frequency (RF) data from the 3D scan for offline processing.

B. Multi-frequency Shear Wave Imaging

In our previous work with the x-MATRIX array, a single frequency 3D shear wave image was achieved by sampling the tissue displacement with the 3D CPA scan sequence available with the X6-1. To enable mutli-frequency shear wave imaging, we modified the CPA sequence based on the sector subdivision method developed by Baghani *et al.* [5]. The number of pulse repetitions (RF samples) per sub-sector was increased from 9 to 16. With a sampling frequency of $f_s = 250$ Hz, the fundamental frequency is reduced to $f_0 = f_s/16 = 15.625$ Hz. With such a frequency resolution, we were able to capture

the shear wave response to three excitation frequencies simultaneously, e.g., $[40, 50, 60]$ Hz, or $[45, 55, 65]$ Hz. To limit the overall scan time of a 3D CPA sweep, the scan depth is set to 16 cm with a 2D plane refresh rate of 2 Hz. The transducer is programmed to repeat this sequence for all 24 elevation planes in a 40° sector sweep, resulting in a large FOV 3D volumetric scan that is completed within 12 s.

The relative axial displacements for all scan lines in the 3D imaging volume is estimated using the normalized cross-correlation (NCC) based time delay estimation algorithm developed by Zahiri-Azar *et al.* in [6] with a window size of 1.3 mm. This leads to a tissue displacement time series with 15 samples denoted as $u(t_i)$, with t_i as the time instance and $i = 1 \dots 15$ as the sample index. If we consider that $u(t_i)$ is the sampled real component of the displacement response from a divergence-free shear wave field, we can rewrite the displacement in a polar phasor form as follows:

$$\begin{aligned} u(t_i) &= \sum_{m=1}^{3} Re[A_m e^{j\theta_m} e^{j\omega_m t_i}] \\ &= \sum_{m=1}^{3} \underbrace{A_m \cos(\theta_m)}_{x_m} \cos(\omega_m t_i) \underbrace{-A_m \sin(\theta_m)}_{y_m} \sin(\omega_m t_i) \end{aligned} \tag{1}$$

Here, x_m and y_m are the real and the imaginary component of the phasor at frequency $\omega_m = 2\pi f_m$, respectively. $m = 1, 2, 3$ denotes the three different external (shear wave) excitation frequencies. $A_m = \sqrt{x_m^2 + y_m^2}$ and $\theta_m = \arctan(y_m/x_m)$ are corresponding phasor amplitude and phase, respectively. Then, for each displacement voxel, the phasor for each excitation frequency is given by:

$$U_m = x_m + jy_m = A_m e^{j\theta_m} \tag{2}$$

As the gaps between the three vibration frequencies we used are smaller than the fundamental frequency, the standard discrete time Fourier transform (DTFT) is not suitable for recovering the phasors at different frequencies. Instead, because we know f_m and t_i, linear regression can be applied to isolate the response of the carrier frequencies. The regressor Φ is formulated as the following Equation (3):

$$\Phi = \begin{bmatrix} \cos(\omega_1 t_1),\ \sin(\omega_1 t_1), \dots, \cos(\omega_3 t_1),\ \sin(\omega_3 t_1), 1 \\ \vdots \quad \vdots \quad \vdots \quad \vdots \quad \vdots \quad \vdots \\ \cos(\omega_1 t_{15}), \sin(\omega_1 t_{15}), \dots, \cos(\omega_3 t_{15}), \sin(\omega_3 t_{15}), 1 \end{bmatrix} \tag{3}$$

where the last column of ones is used to carry out the bias. It can be shown that Φ is full column rank when the frequencies ω_m are different. $\hat{X} = [x_1, y_1, x_2, y_2, x_3, y_3, \epsilon]^T$ denotes the array of predicted phasor parameters with ϵ as the bias term. By storing the displacement time series in an array form $\boldsymbol{u} = [u_1, \dots, u_i]^T$, we obtain the least square solution of the phasor parameters as $\hat{X} = (M^T M)^{-1} M^T \boldsymbol{u}$.

Due to the inherent time delay of transducer's transmit receive (Tx) cycle, the phasor volume will have phase discontinuities causing spatial artifacts. Proper time delay compensation needs to be applied to synchronize the phasor volume. To track the time delay of each scan line in our 3D scan sequence, all 2D scan planes are indexed with c, and sectors in each scan plane are index with b, each of which has a scan lines. We then compensate the time delay of each scan line relative to the first line in the 3D volume as shown in the following Equation (4):

$$\begin{aligned} \hat{U}_{m(a,b,c)} = U_{m(a,b,c)} &\cdot e^{j\omega_m T_{\text{line}}(a-1)} && \text{(Inter-line)} \\ &\cdot e^{j\omega_m T_{\text{line}} a(b-1)16} && \text{(Inter-sector)} \\ &\cdot e^{j\omega_m T_{\text{line}} ab(c-1)16} && \text{(Inter-plane)} \end{aligned} \tag{4}$$

Here, $T_{\text{line}} = \Delta t_i$ is the time of each Tx cycle. The synchronized phasor volumes are scan-converted based on the transducer specifications and spatially interpolated with a grid size of $0.6 \times 0.6 \times 0.6$ mm^3 in the Cartesian coordinate system.

C. Elasticity Reconstruction

The local frequency estimation (LFE) algorithm [7] is used to compute the spatial wavelength in the shear wave pattern and to estimate the elasticity at each excitation frequency. Before applying the reconstruction, a 3D phasor volume is first converted into the spatial frequency domain via the fast Fourier transform (FFT) algorithm where a 6^{th} order Butterworth band-pass filter is applied to reduce the spatial noise. The cutoff frequencies were set to exclude any frequency content that is irrelevant to the range of the elasticity measurement, i.e. Youngs modulus below 1 kPa or above 50 kPa. As suggested by Manduca *et al.* in [7], directional filtering along the 6 orthogonal axes is combined with 3D LFE algorithm to ensure that wave pattern can be captured in all directions. With the estimated local wave length $\hat{\lambda}_m$ for a given excitation frequency, the following simplified solution of the linear elasticity equation was used to approximate the Youngs modulus (E) is the unit of kPa as:

$$\hat{E} \approx \frac{3\rho}{m} \sum^{m} \frac{f_m^2}{\hat{\lambda}_m^2} \tag{5}$$

Here, ρ is the tissue mass density, where we used the density of water, i.e. $\rho = 1\text{kg/m}^3$, as an approximation. Note that the finalized elasticity measurement is the weighted average from all three excitation frequencies.

D. Phantom Characterization

The system was validated with the shear wave liver fibrosis phantom package (Model 039, Elasticity QA Phantom, CIRS, Norfolk. VA). The elasticity of the first three phantoms in the package, where the factory reported elasticity values are given as 5 kPa, 13 kPa, and 25 kPa, respectively, were measured. During the experiment, each phantom was placed on top of the shaker board while the excitation was active. Data from freehand 3D scans were collected to reconstruct the phantom elasticity maps. The base-line reference we used was from the 3D MRE data collected at the UBC MRI research center. To avoid the measurement bias, the MRE measurements were generated from the LFE algorithm with the same settings as we used for S-WAVE.

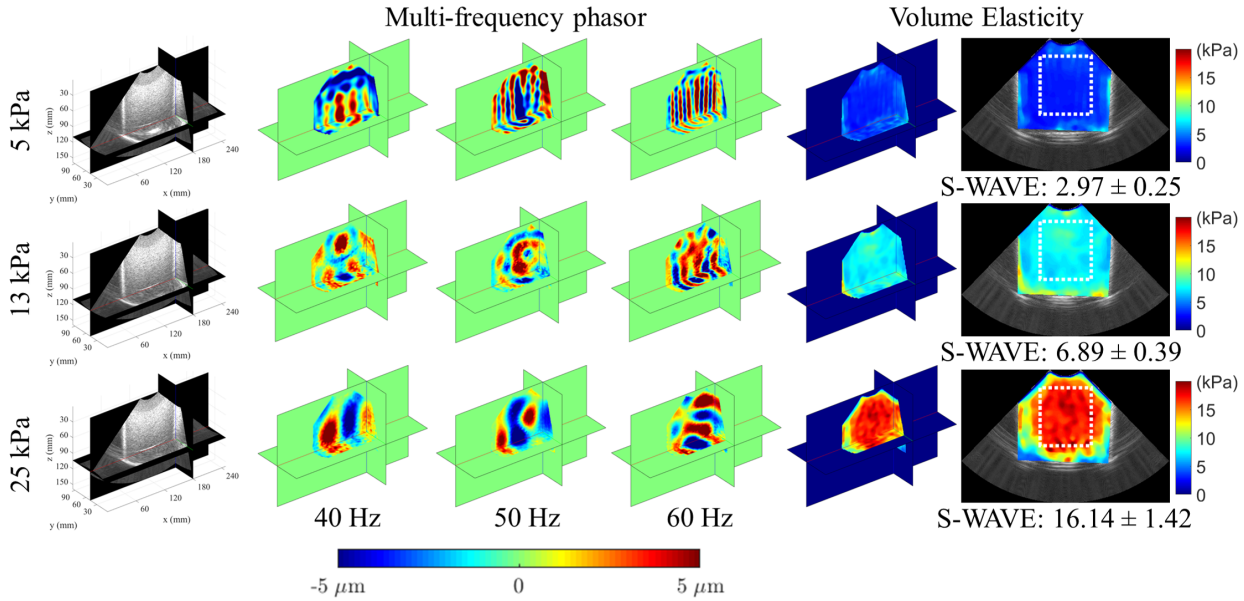

Fig. 1: S-WAVE Phantom validation: Image data for phantoms with different stiffness are shown in three rows, where the 3D orthogonal slices of the reconstructed B-mode (left), multi-frequency phasor of 40-50-60 Hz (mid), and elasticity map (right) are provided, respectively. The right column shows the mid-plane 2D slice of the elasticity map, where the mean and standard deviation the highlighted ROIs are reported.

E. In-vivo Study

With approval from the UBC Clinical Research Ethics Board, six healthy volunteers and six patients who have chronic liver diseases (one HBV, three HCV and two NAFLD) were consented and recruited to undergo MRE and S-WAVE scans. All subjects have completed a FibroScan exam at most two months before participating our study. For each subject, the MRE and S-WAVE scans were completed within a single visit of 2 hrs. All subjects were instructed to fast for 3 hrs before attending the appointment. The MRE exams of five healthy volunteers and three patients whose body to mass index (BMI) were below 30 were performed on a 3T Achieva scanner (Philips Healthcare, Best, Netherlands). The mechanical excitation is driven by a custom-designed, concentric coil based chest shaking mechanism [8]. 3D phasors at 50-55-60-65 Hz were captured using the fractionally encoded steady state gradient echo sequence developed in [9]. For the other three patients and one healthy volunteer whose BMI was greater than 30, the commercial MRE system (Resoundant, Rochester, MN), running on a Ingenia Elition 3T X scanner (Philips Healthcare, Best, Netherlands) was applied to obtain base-line hepatic stiffness measurements.

During the 3D S-WAVE exam, the volunteer laid supine on the examination bed with the back coupled to the shaker board and the right arm abducted. For each measurement, the sonographer first positioned the transducer at the intercostal spaces to locate a desired liver screening region with B-mode imaging. Then the operator activated the shaker board and started the data collection. For each scan, the subject was instructed to perform a 12 s inhale breath hold until the sweep was completed. For each subject, three repeated measurements for 40-50-60 Hz and 45-55-65 Hz were taken.

III. Results

Phantom results are presented graphically in Figure 1. The 3D orthogonal slices of the reconstructed multi-frequency phasor volumes show that our system was able to recover the shear wave pattern in tissue at different excitation frequencies. A 3D ROI at the imaging volume center, with a dimension of 6 cm (X) $\times$ 6 cm (Y) $\times$ 3 cm (Z), is cropped to sample the elasticity readings. Table I lists the measurements obtained with MRE and S-WAVE. According to the results, S-WAVE produces similar readings for the three phantoms of different stiffness with an average variation below 0.5 kPa.

Figure 2 presents example images we collected from the *in vivo* study. To ensure the hepatic stiffness readings were generated from the same tissue region in both imaging modalities, each subject's MRE and S-WAVE data were aligned using the B-mode and T1 volumes via rigid registration, where the hepatic and portal veins, as well as the gallbladder, were manually selected and used as fiducial markers. In each pair of aligned imaging volumes, the 3D ROIs were then manually selected at the same location as shown in Figure 2. The elasticity mean and the standard deviation within the ROI were then reported.

The elasticity results are summarized as a scatter plot shown in Figure 3, where each sample is based on the patient's average hepatic stiffness reported by MRE and S-WAVE. The FibroScan results of all subjects are presented in a similar fashion using MRE as the reference. S-WAVE was able to

TABLE I
TISSUE PHANTOM CALIBRATION RESULTS

Methods	Soft (kPa)	Medium (kPa)	Hard (kPa)
MRE	2.82 $\pm$ 0.25	6.56 $\pm$ 0.32	15.67 $\pm$ 0.33
S-WAVE	2.97 $\pm$ 0.25	6.89 $\pm$ 0.39	16.14 $\pm$ 1.42

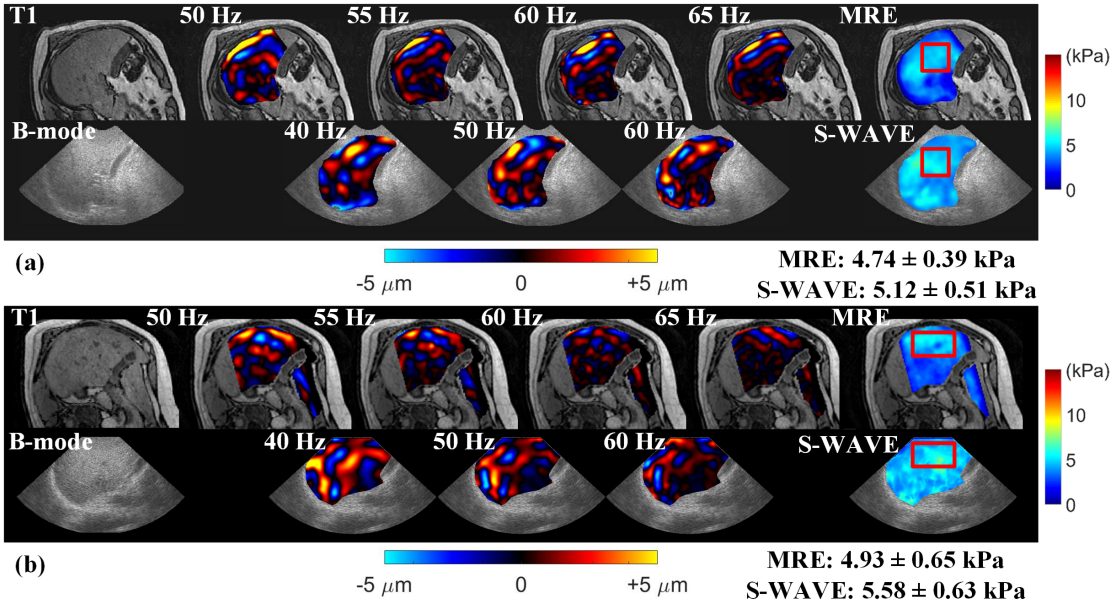

Fig. 2: In-vivo validation data example: (a) Registered MRE and S-WAVE data for healthy volunteer #3. The center slice of the aligned imaging volumes, including B-mode, T1, shear wave phasor amplitude overlays, and elasticity overlay are presented, respectively. (b) An example of the registered data of patient #2 (treated HCV) are presented in a similar fashion. In both cases, the measurement ROI is highlighted by a red rectangle, where the mean and standard deviation of the elasticity values are reported.

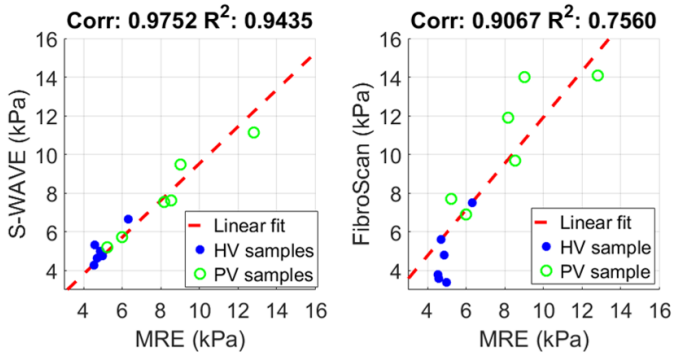

Fig. 3: *In vivo* measurement comparison results. Left: S-WAVE vs MRE, where the best fitted line, $E_{\text{S-WAVE}} = 0.9538 \times E_{\text{MRE}}$ (kPA), is highlighted in red. Right: FibroScan vs MRE, where the best fitted line is obtained as $E_{\text{Fibro}} = 1.1933 \times E_{\text{MRE}}$ (kPA).

achieve a cross-correlation above 97% when compared to MRE with a R-square value above 0.94 for the linear fit. Compared to the results reported by FibroScan, S-WAVE has the advantage of achieving a more consistent agreement to the MRE baseline.

IV. Conclusion

In this work, we presented an implementation of our multi-frequency 3D S-WAVE technique with a matrix array transducer. The system performance was characterized in tissue phantoms and in a preliminary *in vivo* study with six healthy volunteers and six patients who had chronic liver diseases. Experimental results show that S-WAVE with xMATRIX is able to generate reliable quantitative hepatic stiffness measurements which are better correlated to MRE than the results from transient elastography. Further investigation on quantifying liver tissue viscosity with 3D multi-frequency S-WAVE is warranted.

References

[1] A. M. Kevin J. Glaser and R. L. Ehman, "Review of MR elastography applications and recent developments," *J. Magn. Reson. Imaging*, vol. 36, no. 4, pp. 757–774, 2012.

[2] R. G. Barr, G. Ferraioliand, M. L. Palmeri, Z. D. Goodman, G. Garcia-Tsao, J. Rubin, B. Garra, R. P. Myers, S. R. Wilson, D. Rubens, and D. Levine, "Elastography assessment of liver fibrosis: Society of radiologists in ultrasound consensus conference statement," *Radiology*, vol. 276, no. 3, pp. 845–861, 2015.

[3] J. Abeysekera, R. Rohling, and S. Salcudean, "Vibro-elastography: Absolute elasticity from motorized 3D ultrasound measurements of harmonic motion vectors," in *Proc. - 2015 IEEE Int. Ultrason. Symp.*, 2015, pp. 1–4.

[4] Q. Zeng, M. Honarvar, J. Lobo, C. Schneider, R. Rohling, A. Agarwal, G. Harrison, C. Hu, S. Dianis, J. Jago, and S. E. Salcudean, "3D liver shear wave absolute vibro-elastography with an xmatrix array - a healthy volunteer study," in *Proc. - 2018 IEEE Int. Ultrason. Symp.*, 2018, pp. 1–9.

[5] A. Baghani, A. Brant, S. E. Salcudean, and R. Rohling, "A high-frame-rate ultrasound system for the study of tissue motions," *IEEE Trans. Sonics Ultrason.*, vol. 57, no. 7, pp. 1535–1547, 2010.

[6] Z.-A. R and S. E. Salcudean, "Motion estimation in ultrasound images using time domain cross correlation with prior estimates," *IEEE Trans. Biomed. Eng.*, vol. 53, no. 10, pp. 1990–2000, 2006.

[7] A. Manduca, D. S. Lake, S. A. Kruse, and R. L. Ehman, "Spatio-temporal directional filtering for improved inversion of MR elastography images," *Med. Image Anal.*, vol. 7, no. 4, pp. 465–473, 2003.

[8] R. S. Sahebjavaher, S. Frew, A. Bylinskii, L. Beek, P. Garteiser, M. Honarvar, R. Sinkus, and S. Salcudean, "Prostate MR elastography with transperineal electromagnetic actuation and a fast fractionally encoded steady-state gradient echo sequence," *NMR in Biomed*, vol. 27, no. 7, pp. 784–794, 2014.

[9] P. Garteiser, R. S. Sahebjavaher, L. C. Ter Beek, S. Salcudean, V. Vilgrain, B. E. Van Beers, and R. Sinkus, "Rapid acquisition of multifrequency, multislice and multidirectional MR elastography data with a fractionally encoded gradient echo sequence," *NMR in Biomed*, vol. 26, no. 10, pp. 1326–1335, 2013.